2021 American Control Conference (ACC)
New Orleans, USA, May 25-28, 2021

A sparse H_∞ controller synthesis perspective on the reconfiguration of brain networks*

Ilias Mitrai[1], Catherine Stamoulis[2,3] and Prodromos Daoutidis[1]

***Abstract*— Complex networked systems are the norm in the modern world with the human brain being one of the most complex networks. The control of such systems is a difficult task due to the interactions among the individual elements of the system. In this paper the design of sparse feedback controllers for complex networks is considered. Specifically, an $\mathcal{H}_\infty$ controller synthesis problem with D stability constraints is formulated and solved for networks with different topological features. This formulation allows us to examine tradeoffs between control performance, controller sparsity and speed of closed-loop response. We applied this formulation to synthetic networks and the Macaque visual cortical network, assuming Laplacian node dynamics. The results show that as the requested response becomes faster, the control performance improves, and the feedback gain matrix becomes sparser but with larger non-zero entries. This is analogous to the observation that functional brain networks during high cognitive demand adopt a more efficient but also costlier configuration. This analogy suggests a possible connection between cognitive control and closed-loop control under sparse feedback.**

I. INTRODUCTION

Networks are widely used across disciplines to describe interactions between elements of a system [1]. A network can be expressed mathematically by a graph $\mathcal{G}(V, E)$, where V are the nodes (the discrete elements of the system), and E are the edges (the interactions between the nodes). An undirected graph can be represented by a binary or weighted adjacency matrix A. An element (i, j) of a binary A_{ij} is one if node i is connected to node j and zero otherwise. In a weighted A_{ij} matrix, non-zero elements correspond to the strength of the interaction between nodes i and j. The network perspective of a system can provide information about its large scale properties. The analysis of a large-scale networks, e.g. social [2], economic [3], brain [4] and metabolic [5], has revealed common topological features that characterize optimal networks, namely, modular structure, hierarchy, core periphery and small world. These features has been related to efficient network communication [6] and robustness [7]. In this paper we focus on the impact of network topology on the closed-loop control of the system with a specific exponential decay ratio.

The effect of network topology on network control has been analyzed primarily from an open-loop control perspective, focusing on controllability [8], observability [9], selection of driver nodes [10] and minimum energy control [11]. Closed-loop control has also been analyzed for networks with Laplacian dynamics under the sparsity promoting control approach proposed in [12]. The simultaneous optimization of control performance and controller sparsity has shown that under high feedback cost, modular networks lead to lower total cost [13], [14] compared to non-modular ones.

Concepts of network control have also been applied to biological systems, including the brain [15], which is characterized by structural and functional networks. Structural networks provide anatomical information on physical connections (neural fiber tracts - the edges) among different brain regions (nodes) and describe the brain's neuronanatomical architecture. Functional networks provide (co)activation (statistical) information on interactions between different brain regions in response to cognitive demands, and are thus dynamically reconfigured as a function of these demands. Brain network control has been analyzed using linear models [15] focusing on controllability [16] and minimum energy control [17], [18]. Although these approaches provide insights on the selection of driver nodes and minimum transition cost, they treat the control of the brain as an open-loop problem.

In this work we expand the scope of our previous work [13], [14] by considering an $\mathcal{H}_\infty$ sparse controller synthesis problem under additional D stability constraints. We consider synthetic brain networks with Laplacian node dynamics. We find that a restriction of the eigenvalues of the closed-loop system leads to a change in the structure of the optimal feedback gain matrix K, which depends on the graph structure. We note qualitative analogies between changes in the feedback matrix K for different D stability constraints and the observed reconfiguration of brain networks during low and high cognitive demands. These analogies suggest a possible connection between functional brain networks and closed-loop control under sparse feedback.

II. FORMULATION OF THE $\mathcal{H}_\infty$ OPTIMAL SPARSE CONTROLLER SYNTHESIS PROBLEM WITH D STABILITY CONSTRAINTS

We consider a network that is represented by a graph $\mathcal{G}(V, E)$ with n nodes. We assume Laplacian dynamics on the graph, i.e. the evolution of the state of node i depends on the discrepancies between states at adjacent nodes, described by the following equations:

$$\begin{aligned} \dot{x}(t) &= -Lx(t) + B_2u(t) + B_1w(t) \\ y(t) &= Cx(t) \end{aligned} \quad (1)$$

* This work is supported by NSF OAC (award numbers 1938914 and 1940096).

[1] Department of Chemical Engineering and Materials Science, University of Minnesota, Minneapolis, MN 55414, USA.

[2] Department of Medicine, Harvard Medical School, [3]Boston Children's Hospital, Boston MA, 02115, USA.

P. Daoutidis is the corresponding author. daout001@umn.edu

where $x \in \mathbf{R}^n$ are the states of the system (state x_i corresponds to node i), $y \in \mathbf{R}^n$ are the measured/controlled outputs, $u \in \mathbf{R}^n$ are the control inputs, $w \in \mathbf{R}^n$ are the exogenous disturbances, $B_1 \in \mathbf{R}^{n\times n}, B_2 \in \mathbf{R}^{n\times n}, C \in \mathbf{R}^{n\times n}$ and $L \in \mathbf{R}^{n\times n}$ is the Laplacian matrix of the graph, which is equal to:

$$L = D - A \tag{2}$$

where $D = \text{diag}(k_1, ..., k_n)$ is a diagonal matrix (k_i is the degree of node i) and A ($A_{ij} = \{0, 1\}$) is the adjacency matrix of the graph. We assume that we can control and measure all the states of the system, hence $B_1 = B_2 = B = C = \mathbf{1}_{n\times n}$, where $\mathbf{1}_{n\times n}, \mathbf{0}_{n\times n}$ is the $n \times n$ identity and zero matrix respectively. We also define the performance vector $z = [Cx(t)\ u(t)]^\top$. The state space realization of the generalized system is:

$$\begin{aligned} \dot{x} &= -Lx(t) + Bu(t) + Bw(t) \\ z(t) &= \begin{bmatrix} C \\ \mathbf{0}_{n\times n} \end{bmatrix} x(t) + \begin{bmatrix} \mathbf{0}_{n\times n} \\ \mathbf{1}_{n\times n} \end{bmatrix} u(t) + \mathbf{0}_{2n\times n} w(t) \\ y(t) &= Cx(t) + \mathbf{0}_{n\times n} w(t) + \mathbf{0}_{n\times n} u(t) \end{aligned} \tag{3}$$

We use full state feedback, hence $u(t) = Kx(t),\ K \in \mathbf{R}^{n\times n}$. The closed-loop dynamics are:

$$\begin{aligned} \dot{x} &= (-L + BK)x(t) + Bw(t) \\ z(t) &= (C_1 + D_{12}K)x(t) + D_{11}w(t) \end{aligned} \tag{4}$$

where

$$\begin{aligned} C_1 &= \begin{bmatrix} C & \mathbf{0}_{n\times n} \end{bmatrix}^\top \in \mathbf{R}^{2n\times n} \\ D_{12} &= \begin{bmatrix} \mathbf{0}_{n\times n} & \mathbf{1}_{n\times n} \end{bmatrix}^T \in \mathbf{R}^{2n\times n} \\ D_{11} &= \mathbf{0}_{2n\times n}, B = \mathbf{1}_{n\times n}. \end{aligned} \tag{5}$$

The $\mathcal{H}_\infty$ sparse controller synthesis problem for this system is presented in Eq. 6. In this problem, the optimization variables are the P matrix ($P = P^\top \in \mathbb{R}^{n\times n}$) which depends on K through the Bounded Real Lemma (first constraint), the bound on the $\mathcal{H}_\infty$ norm γ ($|G|_\infty \leq \gamma$), and the feedback gain matrix K. This formulation incorporates the sparsity term ($|K|_1$) in the objective function. Specifically, p is a parameter (feedback cost) that penalizes the feedback gain matrix and thus promotes sparsity of the controller. The solution of this problem will provide a sparse controller K that will render the closed-loop system stable and will guarantee rejection of exogenous disturbances of all frequencies. A small value of γ indicates satisfactory control performance, since the effect of the disturbances on the output is small, and a large $|K|_1$ indicates high control cost. An additional constraint will be imposed on the dynamic response of the closed-loop system, by placing the poles of the closed-loop system at a specific region of the complex plain. These regions are called D regions and can be described by Linear Matrix Inequalities [19]. In this work we focus on the restriction of the real part of the eigenvalues of the closed-loop system below a certain value $-\alpha$ ($\alpha \geq 0$), $D(\alpha) = \{\lambda \in C : Re(\lambda) < -\alpha\}$.

$$\begin{aligned} &\underset{P,K,\gamma}{\text{minimize}}\ \gamma + p\ |K|_1 \\ &\text{subject to} \begin{bmatrix} P(-L + B_2K) + (-L + BK)^\top P & PB & (C_1 + D_{12}K)^\top \\ B^\top P & -\gamma \mathbf{1}_{n\times n} & D_{11}^\top \\ C_1 + D_{12}K & D_{11} & -\gamma \mathbf{1}_{2n\times 2n} \end{bmatrix} \prec \mathbf{0}_{4n\times 4n} \\ &\qquad P \succ 0, \gamma \geq 0 \end{aligned} \tag{6}$$

This D region can be described by the following D stability constraint [20]:

$$(-L + BK)P + P(-L + BK)^\top \prec -2\alpha P. \tag{7}$$

This D stability constraint along with Eq. 6 forms the $\mathcal{H}_\infty$ sparse controller synthesis problem under D stability constraints. This problem seeks to find a trade-off between control performance (γ) and control cost ($|K|_1$), while promoting sparsity, for a given speed of closed loop response (α). For the solution of this problem, we note that if P (or K) is fixed, the problem is convex with respect to K, γ (or P, γ). This is a bi-convex optimization problem and can be solved using block coordinated descent [21]. All the problems were solved in Python using CVXPY [22], the DCMP package [21] and CVXOPT. Note that the convergence of block coordinate descent is not guaranteed and the solution obtained depends on the initialization of the algorithm.

III. $\mathcal{H}_\infty$ Optimal Sparse Controller Design: Results for Different Structures and D Stability

In this section the optimal sparse controller synthesis problem is solved for different networks, values of the α parameter in the D stability constraint, and values of the p parameter. Three networks are considered with 20 nodes, a random Erdős-Rényi graph, a graph with community and a graph with core periphery structure. The graphs are created using NetworkX [23].

A. Results without the incorporation of the D stability constraint ($\alpha = 0$) (Fig. 1)

1) Erdős-Rényi graph: For this random graph (first column), increasing the parameter p leads to a sparser feedback gain matrix K with lower control cost and worse control performance (γ increases). The feedback matrix does not have an apparent structure. Based on the individual values of K, the control cost for nodes with low degree is higher

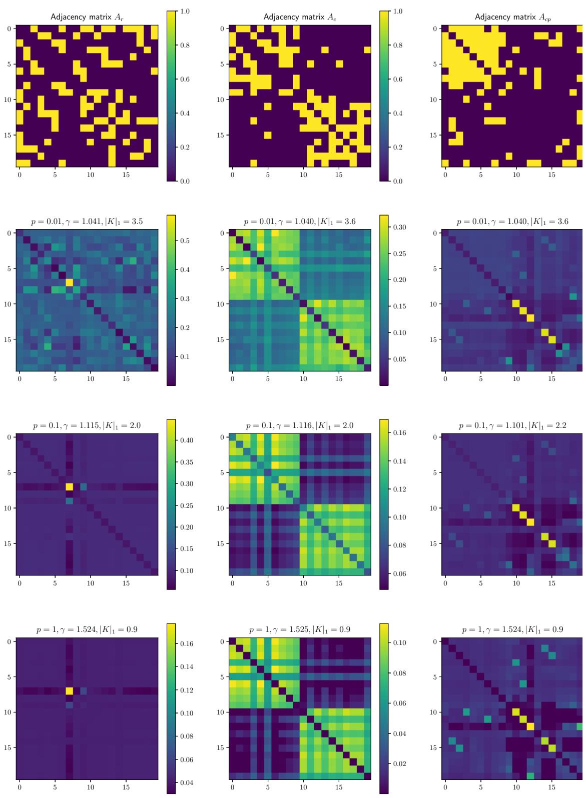

Fig. 1: Optimal sparse controller design (without D stab constraints) for different values of p

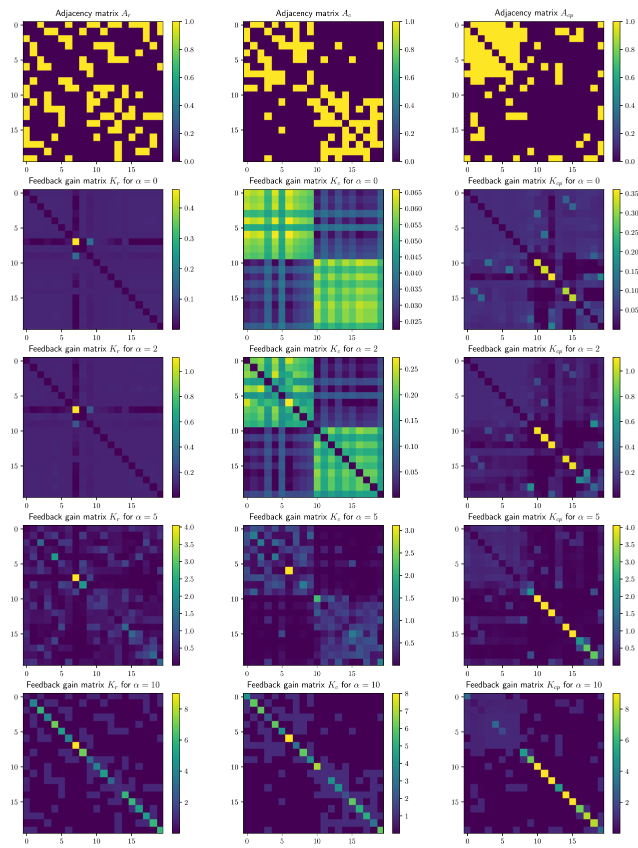

Fig. 2: Sparse feedback gain design results using the D stability constraint. In the first row the adjacency matrices are presented. In the next rows the optimal sparse feedback gain matrix is presented for different values of α (0,2,5,10)

compared to nodes with high degree. This is a consequence of the low connectedness of these nodes which requires more aggressive control action even for small disturbances in order to regulate the node.

2) Graph with community structure: For this case (second column), the feedback gain matrix and the adjacency matrix have similar structure. This arises since the nodes that belong in a community are densely connected, hence control action on a node affects all the other nodes in the community. An increase in the value of p leads to sparser controllers with worse control performance and lower control cost. These results are consistent with [14] where an increase in p was shown to lead to lower inter-community interactions in the K matrix. We note that the control action for the nodes that connect the two communities depends on the state of all the nodes for all the values of the parameter p. We can consider these nodes as coordinators that consider the state of both communities before taking control action.

3) Graph with core periphery structure: In the last graph, the structures of the A_{cp} and K matrix differ and an increase in the p parameter leads to an increase in the sparsity of the controller and decrease in the control cost and performance. Similar to [24], in the K matrix two different patterns can be identified. The control in the core is based on the nodes in the core and the periphery, whereas the control in the periphery depends mainly on the periphery itself.

B. Results with the incorporation of the D stability constraint

In this section, the $\mathcal{H}_\infty$ sparse controller synthesis problem is solved for three types of randomly generated graphs with the same structure as in Section III-A, and the results are presented in Table I. We see that the value of p does not affect the sparsity of the controller when the value of α in the D stability constraint is greater than two. Thus we will fix the value of p at one and analyze the structure of the controller as the value of α increases from 2 to 10. These results are presented in Figure 2.

1) Erdős-Rényi graph: For this graph the results are presented in the first column. As the value of the α parameter increases, the magnitude of the entries of the K matrix increases, the controller is sparser, and the control performance improves (γ decreases, see Table I). Also, for $\alpha = 5$, the structure of the K matrix resembles the structure of the A_r matrix. Finally for $\alpha = 10$ the diagonal entries of the K matrix are much larger than the off-diagonal entries.

2) Graph with community structure: The results of the graph with community structure are presented in the second column. As the value of α increases, the control performance improves (γ is smaller) and the structure of the K matrix is more sparse, with higher non-zero entries, and similar to the adjacency matrix A_c. For $\alpha = 5$ the adjacency matrix A_c

TABLE I: Value of γ, $|K|_1$ for different values of α and p.

Graph	α	$p=0.01$		$p=0.1$		$p=1$	
		γ	$\lvert K\rvert_1$	γ	$\lvert K\rvert_1$	γ	$\lvert K\rvert_1$
Erdős Rényi	0	1.041	3.5	1.115	2	1.524	0.9
	2	1.038	3.9	1.113	2	1.118	2
	5	1.020	5.1	1.020	5	1.020	5
	10	1.008	10	1.008	10	1.008	10
Community	0	1.040	3.6	1.116	2	1.525	0.9
	2	1.040	3.5	1.110	2.1	1.118	2
	5	1.020	5	1.020	5	1.020	5
	10	1.007	10	1.007	10	1.008	10
Core Periphery	0	1.040	3.6	1.101	2.2	1.524	0.9
	2	1.041	3.5	1.114	2	1.118	2
	5	1.020	5.1	1.020	5	1.020	5
	10	1.008	10	1.007	10	1.008	10

and the feedback gain matrix have the greatest resemblance. Finally, for $\alpha = 10$, the diagonal entries of the K matrix are higher than the off-diagonal entries.

3) Graph with core periphery structure: The results for the graph with core periphery are presented in the last column. For small values of α $(0, 2, 5)$ the results follow the same pattern as before. Initially the control action (in terms of magnitude of the elements in K) is higher for the nodes in the periphery. As α increases, the feedback gain matrix K becomes sparser with larger nonzero entries and the control performance improves. However, unlike the two previous cases, for $\alpha = 10$ the part of the K matrix that corresponds to the nodes in the periphery is sparse, with large non-zero entries, whereas the part corresponding to the core is dense with lower values. This result indicates that high connectedness of the core leads to a centralized type of control for the core nodes.

C. Comparison of the results for all the structures

The values of γ and $|K|_1$ for the different networks and values of α and p are presented in Table I. The values of γ for all the networks are similar for a given value of α. Additionally, for fixed p faster response leads to a sparser controller whose structure depends on the structure of the graph. The main observation is that for the Erdős-Rényi and the community structure graph, as the value of the α parameter increases, the structure of the K matrix transitions from a 'centralized' to a 'distributed' and finally to a 'decentralized' type of control. We define the different types of control as follows:

- Centralized control: The control action in a node is based on the state of the other nodes in the graph, not necessarily in the same block or group, i.e. community or core $(u_i(t) = \sum_{j=1}^{n} K_{ij} x_j(t))$.
- Distributed control: In this case the control action in a node is based on the value of the state of neighbor nodes or nodes in the same block $(u_i(t) \approx \sum_{j \in \mathcal{N}} K_{ij} x_j(t)$, $\mathcal{N}$ is a subset of the nodes).
- Decentralized control: In this case the control action in a node is based on the value of the state that corresponds to the node itself $(u_i(t) \approx K_{ii} x_i(t))$.

For small α, the control action on a node ($u_i = K_i x$, where K_i is the i^{th} row of the matrix) is computed based on the information from many states. As α increases the control action depends only on the state value of the neighbors, and finally for $\alpha = 10$ the control action is essentially taken based only on the value of the state itself ($K_{ii} >> K_{ij}$). The results for the graph with core periphery show the same trend only for $\alpha = 0, 2, 5$. For $\alpha = 10$, the structure of the K matrix changes only for the peripheral nodes. In this case the system is controlled with two different modes. For the core nodes the control is locally 'centralized' and the control action for each core node is based on the state value of the other core nodes. In the periphery we have 'decentralized' control, where the control action on each peripheral node is based on the value of the state itself. This result shows that although the control action for the core is low, the communication burden is higher since the control action in the core nodes requires the information of the states of the other nodes in the core.

Overall, we find that independently of the topology of the graph, large values of α lead to high control cost ($|K|_1$). However, the structure of the K matrix depends on the structure of the graph, since large graph density leads to centralized type of control whereas low density leads to decentralized control. The different control modes exhibit different communication burdens, since in centralized control the exchange of information between the nodes is higher compared to distributed control.

IV. Application to a brain network

Using the work in [25] as the basis of our simulations, in this section the $\mathcal{H}_\infty$ sparse controller synthesis problem under D stability constraints will be solved for a network that resembles the Macaque visual cortical network. Application of community detection shows two communities, but the structure of the graph is different than the graphs with community structure considered in Section III, since more edges *between* communities are present. This simulated network has 30 nodes, each representing a region of the visual system, and 311 edges. Although structural networks do not change dynamically (except at scales much longer than the millisecond time scale of neural dynamics, i.e., developmental scales that are of the order of years), functional networks do and are anatomically constrained by structural connections. So, assuming that there are functional configurations where all structural connections are actively processing information (and thus functional connections have comparable activation strength) in our simulations we impose Laplacian dynamics to the network. Although clearly an over-simplification of true neural dynamics, in the context of this preliminary work this is a reasonable assumption. The control task is to find a sparse controller K such that the system is regulated at $y = 0$ with a specified exponential decay ratio (D stability). This state ($y = 0$) can be considered as the equilibrium state of the network when a specific task is performed. The controller synthesis problem is solved for $\alpha = 2, 5, 10$ and the results are presented in Fig. 3.

For slow response ($\alpha = 2$), the structure of the feedback gain matrix is similar to the structure of the graph and the

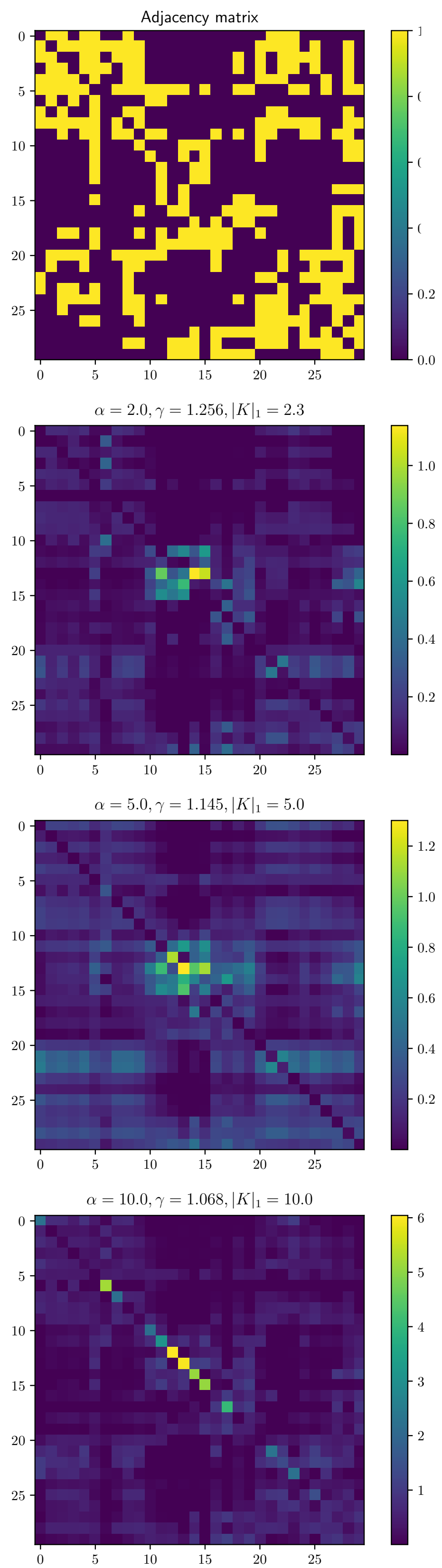

Fig. 3: Feedback gain matrices for the Macaque visual cortical network for different values of α $(2, 5, 10)$

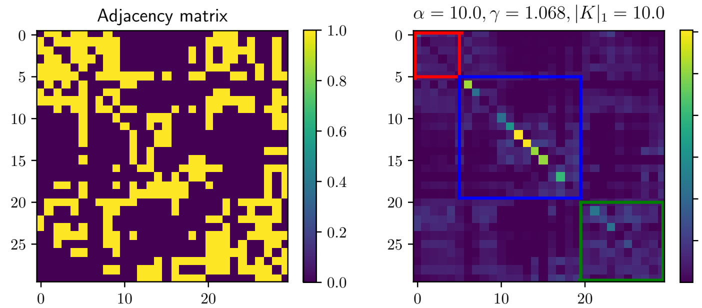

Fig. 4: Feedback gain matrices for the Macaque visual cortical network for $\alpha = 10$. The highlighted regions correspond to different control modes as defined in Section III-C.

control action is concentrated inside the communities. An increase in the speed of response ($\alpha = 5$) leads to a less sparse feedback gain matrix with higher inter-community interactions and better control performance (γ is reduced). Finally, for very fast response ($\alpha = 10$) the K matrix becomes sparser and three different regions can be identified. From Fig. 4, for the nodes that belong in the red and green blocks, the control action depends on the neighbors, whereas for the nodes in the blue block the control action depends mainly on the state of the node itself. These results are in line with the previous observations that larger value of α results in higher control cost and lower local graph density leads to decentralized type of control.

V. Analogies between sparse controller design and brain network reconfiguration

Based on the above results, we can draw some analogies on qualitative trends we observe in the K matrix for different values of α and prior work on the reconfiguration of functional brain networks, and the brain's closed-loop behavior. Assuming Laplacian dynamics and state feedback control, the closed-loop dynamics of brain region i with state x_i has the form:

$$\dot{x}_i(t) = (-L_{ii} + K_{ii})x_i(t) + \sum_{j \neq i}(-L_{ij} + K_{ij})x_j(t). \quad (8)$$

The evolution of state x_i depends on the state itself through $-L_{ii} + K_{ii}$ and on state x_j through $-L_{ij} + K_{ij}$. This summation provides information about the structural coupling $(-L_{ij})$ which is fixed, and the controller coupling (K_{ij}) which is case specific. The feedback gain matrix K captures the interactions among the brain regions, i.e. nodes in the brain network, for a specific control task.

Given this interpretation, we can connect our results from Section IV with the reconfiguration of functional brain networks documented in literature. In [26], [27] it is stated that in response to high cognitive demands, functional networks adopt a more efficient but costlier configuration compared to processes involving low cognitive demands, i.e. the brain seeks a trade-off between wiring cost and information carried between the nodes. This is consistent with the previous observations where it was noted that $\alpha = 5$ guarantees fast rejection of a perturbation, i.e. the network is more efficient, but the control cost $(|K|_1)$ is higher, i.e. the feedback gain matrix is less sparse with higher nonzero entries. On the contrary, a low value of α $(\alpha = 2)$ leads to lower control cost, worse performance and a sparser feedback gain matrix K. Overall, we can consider the case where cognitive demands are low, as the case with low value of α and low control cost $(|K|_1)$ and performance (large γ), and the case of high cognitive demand as the case where α is larger and we have better control performance (γ is lower) and large control cost $(|K|_1)$. Thus, the reconfiguration of functional brain networks during a task may be analogous to a change of the feedback gain matrix which solves an optimal sparse controller synthesis problem under D stability constraints. This analogy suggests a functional brain network may be considered as a closed-loop system $(-L + K)$, combining structural $(-L)$ and case specific (K) interactions among brain regions.

VI. Conclusion

In this paper the effect of the structure of a network on its closed-loop control was analyzed by considering simultaneously the control performance, control cost and speed of closed-loop response. We found that the restriction of the eigenvalues of the closed-loop system leads to a change in the feedback gain matrix K, which depends on the structure of the network. Specifically, for modular and Erdős-Rényi graphs, a transition from a distributed control mode with low control cost to a decentralized type of control with large control cost is observed as the speed of response increases. For networks with core periphery structure, fast response results in two different structures in the feedback matrix K, namely the control in the core nodes is centralized whereas in the periphery decentralized.

A simulated brain network was also examined with simplified (Laplacian) dynamics, and a conceptual relation between the optimal sparse controller synthesis and network topology reconfiguration was proposed. Specifically, we showed that the reconfiguration of brain networks between high and low cognitive demand, shares analogies with the change of the feedback gain matrix resulting from an $\mathcal{H}_\infty$ sparse controller synthesis problem under D stability constraints. This lends itself to an interpretation of the observed change in the functional network in terms of the control cost and performance subject to sparse $\mathcal{H}_\infty$ control.

References

[1] M. Newman, *Networks*. Oxford university press, 2018.

[2] M. Girvan and M. E. Newman, "Community structure in social and biological networks," *Proceedings of the National Academy of Sciences*, vol. 99, no. 12, pp. 7821–7826, 2002.

[3] F. Schweitzer, G. Fagiolo, D. Sornette, F. Vega-Redondo, A. Vespignani, and D. R. White, "Economic networks: The new challenges," *Science*, vol. 325, no. 5939, pp. 422–425, 2009.

[4] E. Bullmore and O. Sporns, "Complex brain networks: graph theoretical analysis of structural and functional systems," *Nature Reviews Neuroscience*, vol. 10, no. 3, pp. 186–198, 2009.

[5] M. R. Da Silva, H. Ma, and A.-P. Zeng, "Centrality, network capacity, and modularity as parameters to analyze the core-periphery structure in metabolic networks," *Proceedings of the IEEE*, vol. 96, no. 8, pp. 1411–1420, 2008.

[6] D. S. Bassett and E. Bullmore, "Small-world brain networks," *The Neuroscientist*, vol. 12, no. 6, pp. 512–523, 2006.

[7] P. Csermely, A. London, L.-Y. Wu, and B. Uzzi, "Structure and dynamics of core/periphery networks," *Journal of Complex Networks*, vol. 1, no. 2, pp. 93–123, 2013.

[8] Y.-Y. Liu, J.-J. Slotine, and A.-L. Barabási, "Controllability of complex networks," *Nature*, vol. 473, no. 7346, pp. 167–173, 2011.

[9] Y. Liu, J. Slotine, and A. Barabási, "Observability of complex networks," *PNAS*, vol. 110, no. 7, pp. 2460–2465, 2013.

[10] J. Gao, Y.-Y. Liu, R. M. D'souza, and A.-L. Barabási, "Target control of complex networks," *Nature Communications*, vol. 5, no. 1, pp. 1–8, 2014.

[11] G. Lindmark and C. Altafini, "Minimum energy control for complex networks," *Scientific Reports*, vol. 8, no. 1, pp. 1–14, 2018.

[12] F. Lin, M. Fardad, and M. R. Jovanović, "Design of optimal sparse feedback gains via the alternating direction method of multipliers," *IEEE Transactions on Automatic Control*, vol. 58, no. 9, pp. 2426–2431, 2013.

[13] P. H. Constantino, W. Tang, and P. Daoutidis, "Topology effects on sparse control of complex networks with laplacian dynamics," *Scientific Reports*, vol. 9, no. 1, pp. 1–9, 2019.

[14] W. Tang and P. Daoutidis, "The role of community structures in sparse feedback control," in *2018 Annual American Control Conference (ACC)*, pp. 1790–1795, IEEE, 2018.

[15] E. Tang and D. S. Bassett, "Colloquium: Control of dynamics in brain networks," *Reviews of Modern Physics*, vol. 90, no. 3, p. 031003, 2018.

[16] S. Gu, F. Pasqualetti, M. Cieslak, Q. K. Telesford, B. Y. Alfred, A. E. Kahn, J. D. Medaglia, J. M. Vettel, M. B. Miller, S. T. Grafton, *et al.*, "Controllability of structural brain networks," *Nature Communications*, vol. 6, no. 1, pp. 1–10, 2015.

[17] S. Gu, R. F. Betzel, M. G. Mattar, M. Cieslak, P. R. Delio, S. T. Grafton, F. Pasqualetti, and D. S. Bassett, "Optimal trajectories of brain state transitions," *Neuroimage*, vol. 148, pp. 305–317, 2017.

[18] R. F. Betzel, S. Gu, J. D. Medaglia, F. Pasqualetti, and D. S. Bassett, "Optimally controlling the human connectome: the role of network topology," *Scientific Reports*, vol. 6, p. 30770, 2016.

[19] M. Chilali and P. Gahinet, "H_∞ design with pole placement constraints: an LMI approach," *IEEE Transactions on Automatic Control*, vol. 41, no. 3, pp. 358–367, 1996.

[20] R. J. Caverly and J. R. Forbes, "LMI properties and applications in systems, stability, and control theory," *arXiv preprint arXiv:1903.08599*, 2019.

[21] X. Shen, S. Diamond, M. Udell, Y. Gu, and S. Boyd, "Disciplined multi-convex programming," in *2017 29th Chinese Control And Decision Conference (CCDC)*, pp. 895–900, IEEE, 2017.

[22] S. Diamond and S. Boyd, "CVXPY: A Python-embedded modeling language for convex optimization," *Journal of Machine Learning Research*, vol. 17, no. 83, pp. 1–5, 2016.

[23] A. Hagberg, P. Swart, and D. S Chult, "Exploring network structure, dynamics, and function using NetworkX," tech. rep., Los Alamos National Lab.(LANL), Los Alamos, NM (United States), 2008.

[24] I. Mitrai, W. Tang, and P. Daoutidis, *Book of Abstracts for the 8th International Conference on Complex Networks & their Applications: COMPLEX NETWORKS 2019*, ch. Control of core-periphery networks under sparse feedback controllers, pp. 585–587. International Conference on Complex Networks & Their Applications, 2019.

[25] O. Sporns and J. D. Zwi, "The small world of the cerebral cortex," *Neuroinformatics*, vol. 2, no. 2, pp. 145–162, 2004.

[26] E. Bullmore and O. Sporns, "The economy of brain network organization," *Nature Reviews Neuroscience*, vol. 13, no. 5, pp. 336–349, 2012.

[27] M. G. Kitzbichler, R. N. Henson, M. L. Smith, P. J. Nathan, and E. T. Bullmore, "Cognitive effort drives workspace configuration of human brain functional networks," *Journal of Neuroscience*, vol. 31, no. 22, pp. 8259–8270, 2011.